

Supplement of Hydrol. Earth Syst. Sci., 21, 4767–4784, 2017  
<https://doi.org/10.5194/hess-21-4767-2017-supplement>  
© Author(s) 2017. This work is distributed under  
the Creative Commons Attribution 3.0 License.



*Supplement of*

## **Use of reflected GNSS SNR data to retrieve either soil moisture or vegetation height from a wheat crop**

**Sibo Zhang et al.**

*Correspondence to:* Jean-Christophe Calvet ([jean-christophe.calvet@meteo.fr](mailto:jean-christophe.calvet@meteo.fr))

The copyright of individual parts of the supplement might differ from the CC BY 3.0 License.

## Supplement of

# Use of reflected GNSS SNR data to retrieve either soil moisture or vegetation height over a wheat crop

S. Zhang et al.

Correspondence to: J.-C. Calvet (jean-christophe.calvet@meteo.fr)

### Locations of the GPS specular reflection points and first Fresnel zones

Larger variability in GPS sub-daily VSM estimates might originate from the different locations observed. Many local environment factors such as vegetation effects, precipitation, changes in soil roughness and soil composition, can perturb the GPS VSM estimates. During satellite overpasses the observed location changes together with the size of the footprint (the First Fresnel Zone, FFZ) of the GNSS system, in relation to the antenna height and elevation angle range. It might be another cause of the sub-daily variability of VSM estimates. Additionally, issues with the SNR data of the L1 C/A signal and the receiving antenna gain pattern may also affect the VSM estimates. The experiment site of the GPS receiving antenna, and the corresponding specular points and FFZ areas at 5 degrees and at 20 degrees of satellite elevation angles (outer circle and inner circle, respectively) are shown in Fig. S1.

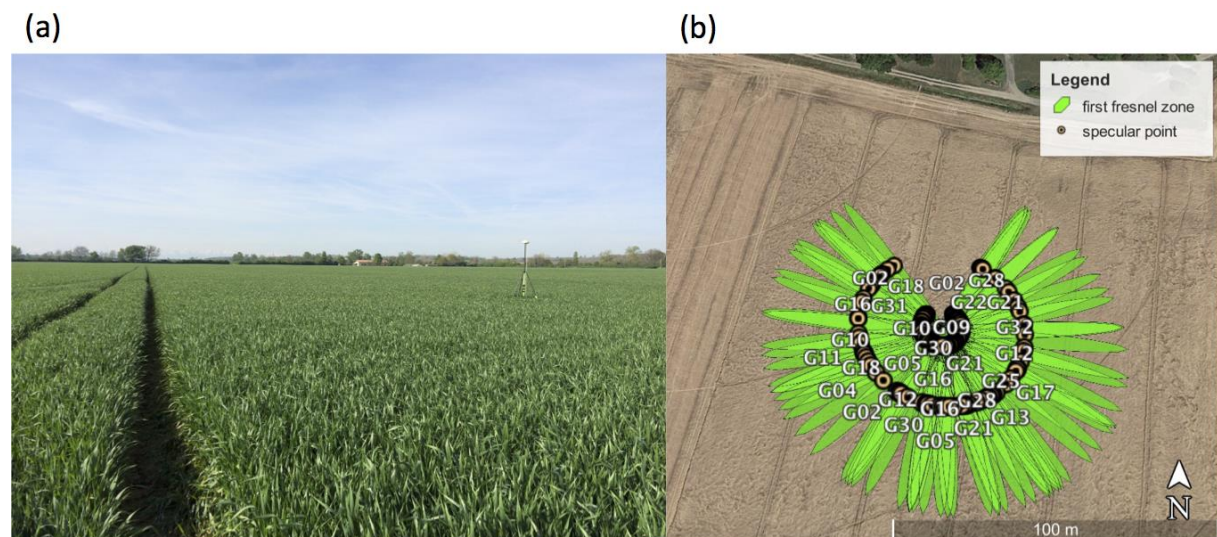


**Figure S1** - (a) Antenna of the GNSS site at 2.51 m above the soil surface over an experimental field covered by rainfed winter wheat in Lamasquère, France ( $43^{\circ}29'10''\text{N}$ ,  $1^{\circ}13'57''\text{E}$ ) on 24 April 2015. (b) Locations of the GPS specular reflection points and first Fresnel zones (FFZ). This simulation is done on 21 January 2015 for satellite elevation angles ranging from 5 to 20 degrees (outer circle and inner circle, respectively). Background geographic information is from Google Earth.

## SNR data

At the Lamasquère site, data from GPS satellites should in theory be received twice per day. However, in practice, some of the satellites were only received once per day.

Figure S2 shows two typical satellite SNR time series for one day (21 January 2015). For GPS01 (top figure), only one ascending track (from low elevation to high elevation) and one descending track (from high elevation to low elevation) were recorded. For GPS18 (bottom figure), there were two ascending tracks and two descending tracks. The observation area (i.e. the reflecting surface) for the ascending track differed from the area seen by the descending track. Thus, we separated the ascending data from data of the descending satellite tracks. For GPS01, we obtained two time series (ascending and descending), and for GPS18 we obtained four time series. Furthermore, GPS01 reached high elevation angles (its maximum elevation angle was about  $77^\circ$ ), making its elevation angle change faster than that of GPS18 (its maximum elevation angles were about  $45^\circ$  and  $29^\circ$ ). Because these differences in maximum satellite elevation angle and elevation angle change rate substantially affected the period of the SNR data, we only used the satellite tracks with at least  $40^\circ$  maximum elevation for retrieving vegetation height. In the case of Fig. S2, this means that we only used the GPS01 track and the morning GPS18 track. The evening GPS18 track was discarded. Then, within selected tracks, only a valid segment SNR data for elevation angles between  $5^\circ$  and  $20^\circ$  were used.

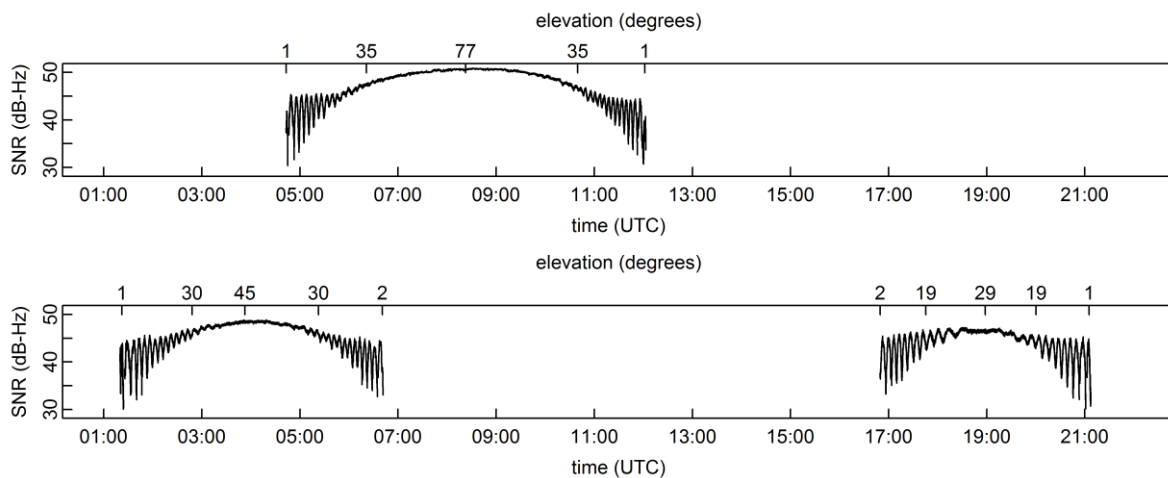


**Figure S2** - Recorded S1C SNR data at Lamasquère for (top) GPS01 and (bottom) GPS18, on 21 January 2015.

## Wavelet Analysis

The WaveletComp R package analyzes the period structure using the "mother" Morlet wavelet (Fig. S3):

$$\psi(t) = \pi^{-1/4} e^{i\omega t} e^{-t^2/2} \quad (\text{S1})$$

The angular frequency  $\omega$  is set to 6, as recommended by Torrence and Compo (1998). The Morlet wavelet transform of the multipath SNR time series ( $\text{SNR}_{\text{mpi}}$ ) is defined as the convolution of the series with a set of "wavelet daughters" generated by the mother wavelet by translation in time by  $\tau$  and scaling by  $s$ :

$$\text{Wave}(\tau, s) = \sum_t \text{SNR}_{\text{mpi}} \frac{1}{\sqrt{s}} \psi^* \left( \frac{t - \tau}{s} \right) \quad (\text{S2})$$

where (\*) denotes the complex conjugate. The localized estimates of the particular daughter wavelet in the time domain is determined by the localizing time parameter  $\tau$  being shifted by a time increment of  $dt$  depending on the sampling interval. The wavelet transform is computed for a wavelet scale ( $s$ ) set of interest, which is a fractional power of 2,

$$s_j = s_{\min} 2^{jd_j}, j = 0, 1, \dots, J \quad (\text{S3})$$

The minimum (maximum) scale is fixed via the choice of the minimum (maximum) period interest depending on the possible relative antenna height change through the conversion factor  $6/(2\pi)$ . In this study they were set as 128 s and 1024 s, respectively. The wavelet transform can be separated into real part and imaginary part, thus providing information on both local amplitude and instantaneous phase of any periodic process across time. The local power of any periodic component of the time series under investigation is

$$\text{Power}(\tau, s) = \frac{1}{s} |\text{Wave}(\tau, s)|^2 \quad (\text{S4})$$

Known as the wavelet power spectrum.

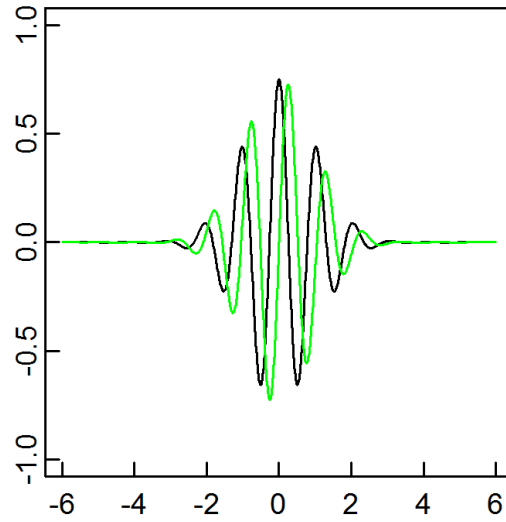


**Figure S3-** The Morlet mother wavelet, real part (black line) and imaginary part (green line)

## References

- Torrence, C., and Compo, G. P.: A practical guide to wavelet analysis, *Bulletin of the American Meteorological Society*, 79(1), 61-78, 1998.
- Roesch, A., Schmidbauer, H., and Roesch, M. A.: 'WaveletComp' package, 2014.

## GDD (growing degree days) model

Temperatures at 2 meter from a large scale simulations made over France with a spatial resolution of 8 km by 8 km were extracted in order to build the growing degree days (GDD) model for Lamasquère site. The reference data was between year 2009 and 2010, it was sown on 1 October 2009, and the tillering, flowering and ripening were on 26 March, 9 June and 12 June 2010, respectively.  $T_{GDD}$  is calculated as the accumulation of daily mean temperatures ( $T_{mean}$ ),  $T_{mean}$  is calculated in the following way:

$$T_{mean} = \frac{T_{max} + T_{min}}{2} - T_{base} \quad (S5)$$

based on the daily minimum ( $T_{min}$ ) and maximum ( $T_{max}$ ) temperatures.  $T_{mean}$  is further forced to range between 0°C and 35°C. The base temperature ( $T_{base}$ ) used here for winter wheat is 0°C and the starting date for the accumulated temperature is from 1 October 2009, the accumulated temperature ( $T_{GDD}$ ) is calculated as

$$T_{GDD} = \sum T_{mean} \quad (S6)$$

This GDD model was applied to year 2015 for our study (Fig. S4), according to the  $T_{GDD}$  in the GDD model, we obtained the following dates for tillering, flowering, and ripening: 12 March, 31 May, and 3 June 2015, respectively.

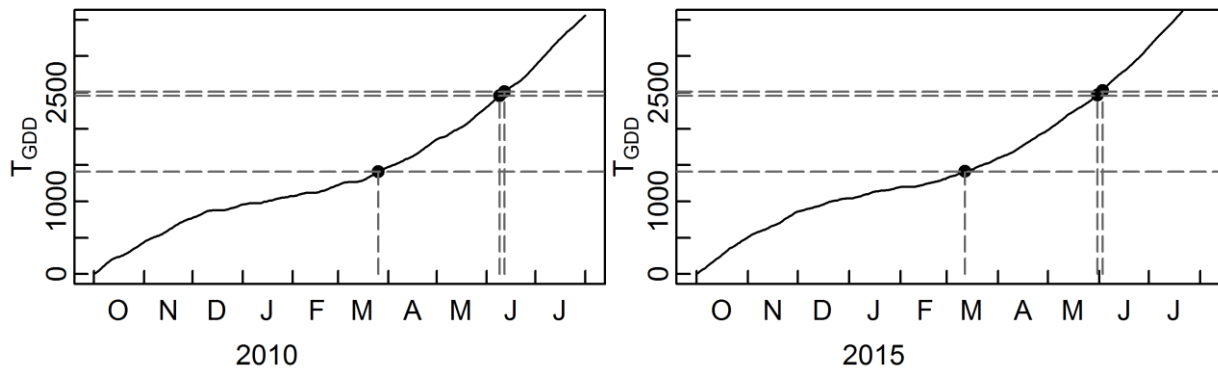


**Figure S4** - (left) The growing degree days (GDD) model build in 2010 for winter wheat at Lamasquère and (right) GDD model build in 2015 at the same site. According to the  $T_{GDD}$  (°C) on the tillering, flowering and ripening in 2010, the corresponding phenological stage dates in 2015 are estimated.

## References

- Betbeder, J., Fieuzal, R., Philippets, Y., Ferro-Famil, L., and Baup, F.: Contribution of multitemporal polarimetric synthetic aperture radar data for monitoring winter wheat and rapeseed crops, *J. Appl. Remote Sens.* 10(2), 026020, doi: 10.1117/1.JRS.10.026020, 2016.
- Duveiller, G., Weiss, M., Baret, F., and Defourny, P.: Retrieving wheat green area index during the growing season from optical time series measurements based on neural network radiative transfer inversion, *Remote Sensing of Environment*, 115(3), 887-896, 2011.

## From phase to volumetric soil moisture

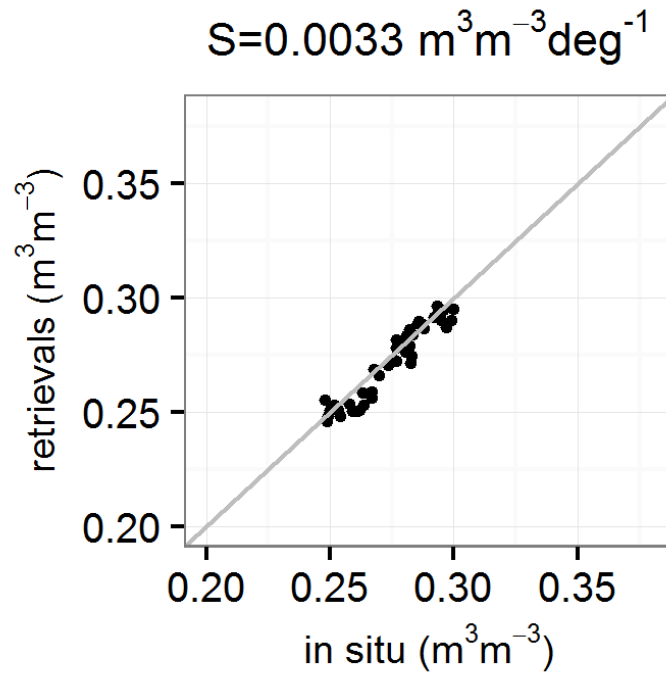


**Figure S5** - Volumetric soil moisture (VSM) GPS retrievals ( $N = 47$ ) versus in situ VSM observations ( $\text{m}^3\text{m}^{-3}$ ) from 16 January to 5 March 2015, with fitted slope =  $0.0033 \text{ m}^3\text{m}^{-3}\text{deg}^{-1}$  for satellite tracks whose phase presents a linear correlation with in situ soil moisture higher than 0.9. This occurred for the ascending tracks of GPS 13, 21, 24, 30 and for the descending tracks of GPS 05, 09, 10, 15, and 23.

## Linear relationship between vegetation height and above-ground dry biomass

We found a good linear relationship between the moving average height from GPS retrievals and the above-ground dry biomass simulated by the ISBA model from 10 March to 29 May 2015 (when the maximum vegetation height, 1 m, was measured), during the time period from tillering to flowering. The correlation coefficient between the moving average height and the above-ground dry biomass, with 81 observations, was 0.996.

$$\text{biomass}_{\text{dry}} = 1.05 \times \text{height}_{\text{moving\_avg}} - 0.19 \quad (\text{S7})$$

with  $\text{biomass}_{\text{dry}}$  (the above-ground dry biomass simulations) in  $\text{kg m}^{-2}$  and  $\text{height}_{\text{moving\_avg}}$  (the moving average height from GPS retrievals) in meter.

A similar result was obtained by Wigneron et al. (2002) over another wheat crop site (*Triticum durum*, cultivar prinqual) in spring 1993 (Fig. S6). Although the sowing date (19 March) was late and the crop cycle was rather short, there was still a very good linear relationship between the in situ wheat height measurements and in situ dry biomass measurements from 20 April to 11 June 1993 (when the maximum vegetation height, 1 m, was measured). The correlation coefficient with 25 observations was 0.996.

$$\text{biomass}_{\text{dry}} = 1.11 \times \text{height} - 0.19 \quad (\text{S8})$$

with  $\text{biomass}_{\text{dry}}$  (in situ above-ground dry biomass measurements) in  $\text{kg m}^{-2}$  and height (in situ measurements) in meter.

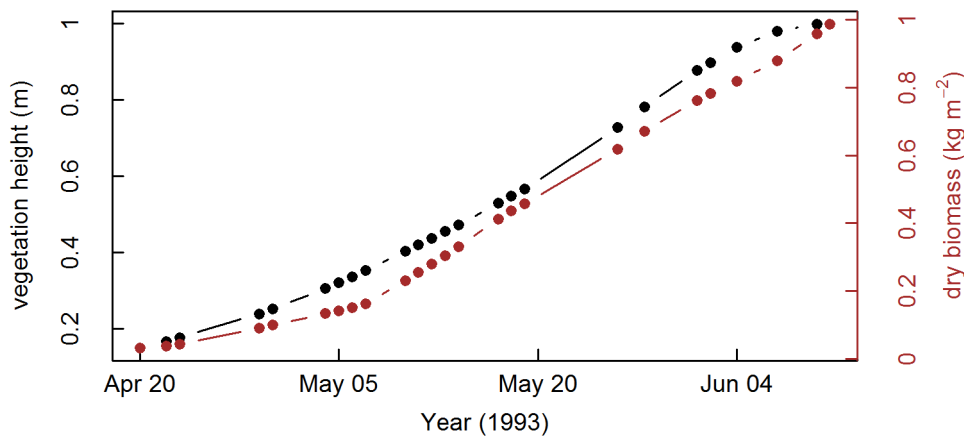


**Figure S6** - In situ wheat canopy height measurements (25 black dots) and in situ wheat above-ground dry biomass measurements (brown dots) from 20 April to 11 June 1993 (adapted from Wigneron et al., 2002).

## Reference

Wigneron, J.P., Chanzy, A., Calvet, J.C., Olioso, A. and Kerr, Y.: Modeling approaches to assimilating L band passive microwave observations over land surfaces, *Journal of Geophysical Research: Atmospheres*, 107(D14), 2002.



**GPS retrieved vegetation height difference**

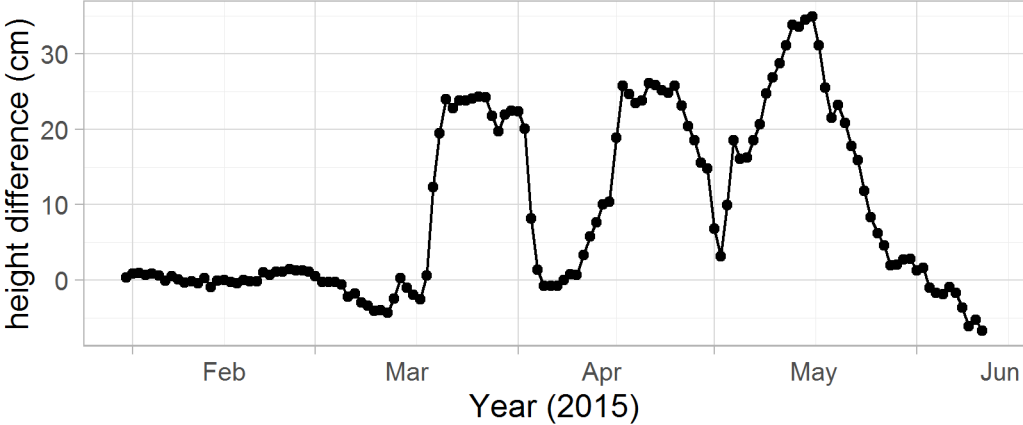


**Figure S7** - The difference between retrieved vegetation height at a given date and retrieved vegetation height 15 days before, from 31 January to 11 June 2015.

## Scores

The mean absolute error (MAE) is a quantity used to measure how close retrievals are to the observations, MAE is given by

$$MAE = \frac{1}{n} \sum_{i=1}^n |VSM_i^{OBS} - VSM_i^{GPS}| \quad (S9)$$

$VSM^{OBS}$  represents the *in situ* VSM observations,  $VSM^{GPS}$  represents the retrieved soil moisture by GPS data, n is the valid number of data.

The root mean square error (RMSE) represents the sample standard deviation of the differences between retrieved values and observed values:

$$RMSE = \sqrt{\frac{\sum_{i=1}^n (VSM_i^{OBS} - VSM_i^{GPS})^2}{n}} \quad (S10)$$

The standard deviation of the difference between observations and retrievals (SDD) is

$$SDD = \sqrt{\frac{\sum_{i=1}^n (x_i - \bar{x})^2}{n}} \quad (S11)$$

$x_i = VSM_i^{GPS} - VSM_i^{OBS}$ ,  $\bar{x}$  is the mean value of x.

The fraction of explained variance is represented by the squared Pearson correlation coefficient,  $R^2$ .